

Supporting Information

Insights into a “seesaw effect” between reducibility and hydrophobicity induced by cobalt doping:

Influence on OMS-2 nanomaterials for catalytic degradation of carcinogenic benzene

Chunlan Ni,^{a,#} Jingtao Hou,^{a,#,*} Qian Zheng,^a Mengqing Wang,^a Lu Ren,^b Mingxia Wang,^a Wenfeng Tan^a

^a State Environmental Protection Key Laboratory of Soil Health and Green Remediation, Hubei Key Laboratory of Soil Environment and Pollution Remediation, College of Resources and Environment, Huazhong Agricultural University, Wuhan 430070, China.

^b School of Civil Engineering, Suzhou University of Science and Technology, Suzhou 215009, China.

These authors contributed equally to the article.

* **Corresponding author:** Jingtao Hou (J. Hou), Email: hout87@163.com.

Text S1. Density Functional Theory (DFT) Calculation

Density functional theory (DFT) calculations were used to investigate the effect of Co ions on the reducibility and hydrophobicity of OMS-2 ($\text{KMn}_8\text{O}_{16}$). The calculations were performed using the Vienna Ab-initio Simulation Package (VASP). The valence electronic states are expanded in a set of periodic plane waves, and the interaction between core electrons and valence electrons is implemented through the projector augmented wave (PAW) approach. The Perdew–Burke–Ernzerhof (PBE) GGA-exchange correlation functional was applied. In relaxation, summations over the Brillouin zone (BZ) are performed with a $2 \times 2 \times 2$ Monkhorst–Pack k-point mesh. The smooth part of the wave functions is expanded in plane waves with a kinetic energy cutoff of 400 eV, and the convergence criteria for the electronic and ionic relaxation are 10^{-4} eV and $0.02 \text{ eV } \text{\AA}^{-1}$, respectively. A supercell of OMS-2 with ~ 100 atoms ($1 \times 1 \times 4$) was constructed and one Co atom was used to replace Mn atom in the supercell. Our calculated lattice parameters of bulk $\text{KMn}_8\text{O}_{16}$ are as follows: $a = 9.755 \text{ \AA}$, and $c = 2.96 \text{ \AA}$.

Text S2. Sample Characterization

The X-ray powder diffraction patterns of catalysts were collected on a Rigaku Dmax X-ray diffractometer using Cu $K\alpha$ radiation. The TEM morphology of catalysts was imaged using a JEM-100CX electron microscope. The BET surface area of catalysts was measured on an ASAP2020 instrument at -196°C . The elemental analysis of catalysts was conducted using an inductively coupled plasma emission spectrometer (ICP-OES, PerkinElmer Optima 4300DV). X-ray photoelectron spectroscopy (XPS) information of the catalysts were recorded on a VG Multilab 2000 X-ray photoelectron spectrometer using Mg $K\alpha$ radiation. The XANES spectra of Co-doped catalyst were collected in fluorescence mode at room temperature on the 1W1B beamline at the Beijing Synchrotron Radiation Facility. The surface hydrophobicity of the catalyst was intuitive characterized by measuring the contact angle in Detaphysics OCA-20. Before testing, powder samples were coated on the side of a double-sided tape uniformly and another side without powder was stuck to the glass slides. Three repeats were carried out for each sample.

The CO temperature-programmed reduction (CO-TPR) experiment was carried out on a TP-5080 multifunctional adsorption apparatus equipped with a TCD detector. To start, 0.0100 g of the catalysts was placed in a quartz reactor. A NaOH particle trap was placed in the front of the detector to adsorb the H_2O and CO_2 . Before the TPR analysis, the catalysts were pretreated in 5 vol % O_2/He at 200°C for 1 h. TPR was performed in a flow of 5 vol % CO/He by heating the pretreated sample (0.0100 g) from room temperature to 700°C with a heating rate of $10^\circ\text{C min}^{-1}$.

Text S3. Catalytic activity test

The catalytic activity tests for complete oxidation of benzene were performed on a WFS-2015 online gas-phase reaction apparatus at temperature from 140 to 260 °C. Typically, the catalyst (0.0500 g) was loaded in the middle of the quartz tube (the inner diameter and length were 16 mm and 600 mm, respectively). A thermocouple was placed inside the quartz tube to monitor the reaction temperature online. The reactor was placed in a temperature-controlled tubular electrical oven. The air stream saturated with the benzene was diluted with another flow of air to yield a final reactant concentration of 2000 mg m⁻³. Figure S1 illustrates the diagram of gas circuit for obtaining the setting humidity and benzene concentration in this study. The saturated water vapor and gas-benzene were obtained through blowing air into a stainless-steel bubbler with containing benzene and water solution, respectively. The flow in the pipe of saturated water vapor was 39.8 mL/min, which was closed to the total flow of 40 mL/min. In the room temperature, the saturated vapor pressure of water is 3.17 kPa. In this case, the calculated absolute humidity in the gas circuit is $39.8/40 \times 3.17 \text{ kPa}/100 \text{ kPa} \approx 3 \text{ vol } \%$. The reactor was connected to a GC9560 gas chromatograph with a flame ionization detector (FID) equipped, an automatically sampling 10-way valve (VALCO) with an air actuator was used. The sampling frequency for GC detection was eight times for each given temperature. The outlet benzene concentration at each given temperature was obtained from the average value of eight collection concentrations.

Table S1 Rietveld structure refinement results of OMS-2 and Co-OMS-2.

Sample	a(Å)	b(Å)	c(Å)	β (°)	Cry size(nm)	Rwp (%)
OMS-2	9.8051(39)	2.8471(11)	9.6170(40)	91.0321(76)	20.60(25)	4.81
CoL-OMS-2	9.844(17)	2.8479(49)	9.623(17)	91.165(11)	14.84(20)	4.80
CoH-OMS-2	9.8357(46)	2.8399(13)	9.6177(48)	91.133(13)	13.48(17)	4.25

Table S2 T_{50} , T_{90} and specific rates of benzene oxidation of the Co-OMS-2.

Sample	Catalytic activity (°C)	
	T_{10}	T_{90}
OMS-2	175	253
Co _L -OMS-2	166	252
Co _H -OMS-2	197	n.d.

Table S3 Summary of the catalytic activity over Mn-based catalysts for benzene oxidation.

Catalysts	Space velocity (mL g _{catalyst} ⁻¹ h ⁻¹)	Benzene concentration	T ₁₀ (°C)	T ₉₀ (°C)	Water resistance test	Ref.
OMS-2	20000	0.9 % in air	~ 180	~ 270	-	1
Ag doped OMS-2	90000	1500 ppm	150-180	220-270	300 °C, 5 vol%	2
Cu-birnessite	120000	410-450 ppm	~175	~325	300°C,RH50%	3
K doped OMS-2	48000	2000 mg m ⁻³	170-245	> 240	-	4
OMS-2	48000	2000 mg m ⁻³	170-220	237-339	-	5
Ag _I /HMO	92000	200 ppm	~160	~ 260	-	6
Fe doped OMS-2	48000	2000 mg m ⁻³	150-180	218-238	-	7
OMS-2	12000	Calculated from saturated vapor pressure at 25 °C	~175	~300	-	8
Ag/OMS-2	360000	2000 ppm	200-215	> 362	-	9
OMS-2	60000	1000 ppm	~ 220	~ 320	-	10
OMS-2	24000	400 ppm	~230	~290	-	11
Co _L -OMS-2	48000	2000 mg m ⁻³	166	252	260 °C, RH3%	This study

References:

- (1) Luo, J.; Zhang, Q.; Garcia-Martinez, J.; Suib, S. L. Adsorptive and Acidic Properties , Reversible Lattice Oxygen Evolution , and Catalytic Mechanism of Cryptomelane-Type Manganese Oxides as Oxidation Catalysts Adsorptive and Acidic Properties , Reversible Lattice Oxygen Evolution , and Catalytic Mechanism . *Journal of the American Chemical Society* **2008**, *130* (5), 3198–3207.
- (2) Deng, H.; Kang, S.; Ma, J.; Zhang, C.; He, H. Silver Incorporated into Cryptomelane-Type Manganese Oxide Boosts the Catalytic Oxidation of Benzene. *Applied Catalysis B: Environmental* **2018**, *239*, 214–222.
- (3) Liu, Y.; Zong, W.; Zhou, H.; Wang, D.; Cao, R.; Zhan, J.; Liu, L.; Jang, B. W. Tuning the Interlayer Cations of Birnessite-Type MnO₂ to Enhance Its Oxidation Ability for Gaseous Benzene with Water Resistance. *Catalysis Science & Technology* **2018**, *8*, 5344–5358.

- (4) Hou, J.; Liu, L.; Li, Y.; Mao, M.; Lv, H.; Zhao, X. Tuning the K⁺ Concentration in the Tunnel of OMS-2 Nanorods Leads to a Significant Enhancement of the Catalytic Activity for Benzene Oxidation. *Environmental Science and Technology* **2013**, *47* (23), 13730–13736.
- (5) Hou, J.; Li, Y.; Liu, L.; Ren, L.; Zhao, X. Effect of Giant Oxygen Vacancy Defects on the Catalytic Oxidation of OMS-2 Nanorods. *Journal of Materials Chemistry A* **2013**, *1* (23), 6736–6741.
- (6) Chen, Y.; Huang, Z.; Zhou, M.; Chen, J.; Tang, X. Single Silver Adatoms on Nanostructured Manganese Oxide Surfaces: Boosting Oxygen Activation for Benzene Abatement. *Environmental Science & Technology* **2017**, *51*, 2304–2311.
- (7) Chen, J.; Li, Y.; Fang, S.; Yang, Y.; Zhao, X. UV–Vis-Infrared Light-Driven Thermocatalytic Abatement of Benzene on Fe Doped OMS-2 Nanorods Enhanced by a Novel Photoactivation. *Chemical Engineering Journal* **2018**, *332*, 205–215.
- (8) Genuino, H. C.; Dharmarathna, S.; Njagi, E. C.; Mei, M. C.; Suib, S. L. Gas-Phase Total Oxidation of Benzene, Toluene, Ethylbenzene, and Xylenes Using Shape-Selective Manganese Oxide and Copper Manganese Oxide Catalysts. *The Journal of Physical Chemistry C* **2012**, *116* (22), 12066–12078.
- (9) Fu, J.; Dong, N.; Ye, Q.; Cheng, S.; Kang, T.; Dai, H. Enhanced Performance of the OMS-2 Catalyst by Ag Loading for the Oxidation of Benzene, Toluene, and Formaldehyde. *New Journal of Chemistry* **2018**, *42*, 18117–18127.
- (10) Li, D.; Yang, J.; Tang, W.; Wu, X.; Wei, L.; Chen, Y. Controlled Synthesis of Hierarchical MnO₂ Microspheres with Hollow Interiors for the Removal of Benzene. *RSC Advances* **2014**, *4*, 26796–26803.
- (11) Hu, Z.; Mi, R.; Yong, X.; Liu, S.; Li, D.; Li, Y.; Zhang, T. Effect of Crystal Phase of MnO₂ with Similar Nanorod-Shaped Morphology on the Catalytic Performance of Benzene Combustion. *ChemistrySelect* **2019**, *4*, 473–480.

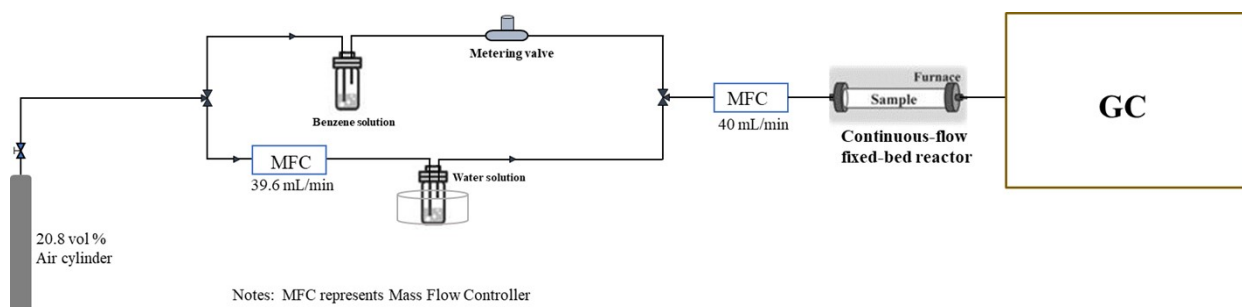


Figure S1 Schematic illustration of gas circuit for obtaining the setting humidity and benzene concentration in this study.

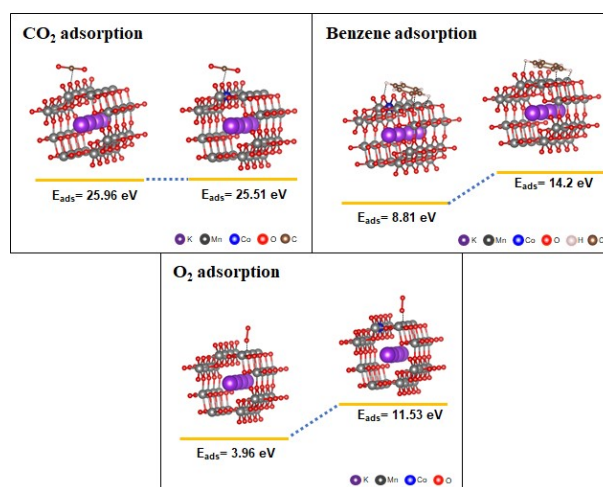


Figure S2 Constructed OMS-2 supercell without ($\text{K}_4\text{Mn}_{32}\text{O}_{64}$) and with 1 atom% Co doping ($\text{K}_4\text{Mn}_{31}\text{Co}_1\text{O}_{64}$) for calculating the energy of CO_2 , benzene, and O_2 adsorption: purple for K, gray for Mn, red for O, blue for Co, white for H, and brown for C.

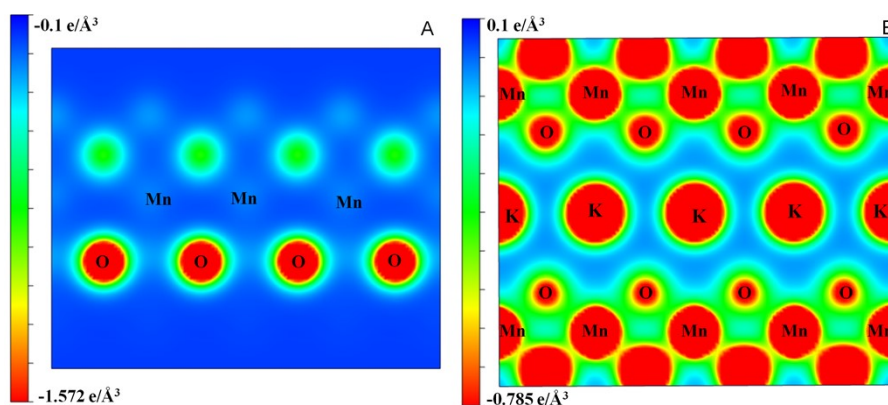


Figure S3 Electron density of one orientation on the surface (A) and bulk (B) of the Co doped OMS-2 supercell: The color scale represents the range of the electron density ($\text{e} \text{\AA}^{-3}$).

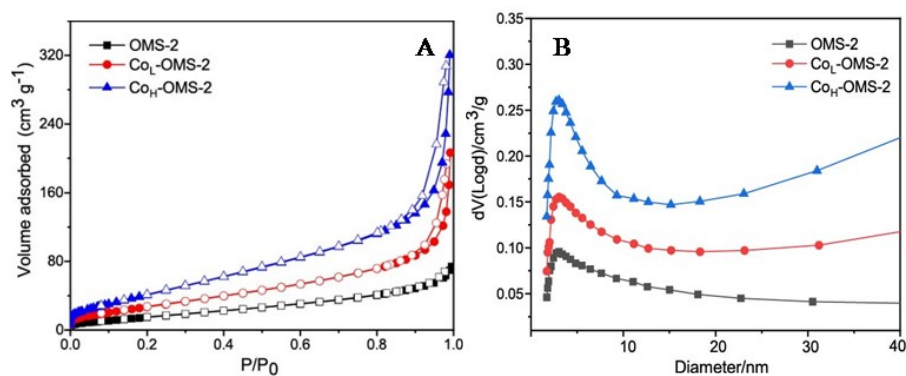


Figure S4 N_2 adsorption-desorption curves (A) and pore diameter distribution curves (B) for pure OMS-2 and Co-OMS-2.

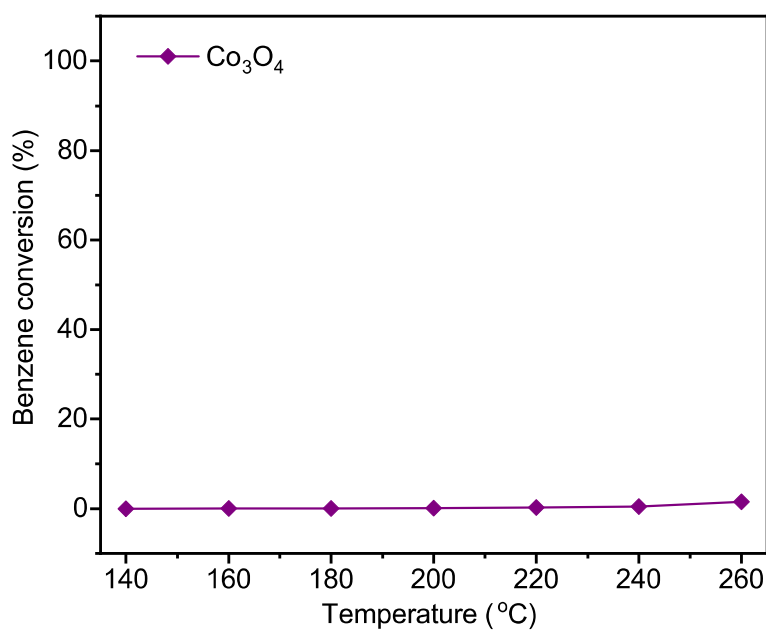


Figure S5 Benzene conversion of Co_3O_4 sample under the condition of benzene concentration = 2000 mg m^{-3} and $\text{SV} = 48000 \text{ mL g}_{\text{catal}}^{-1} \text{ h}^{-1}$.

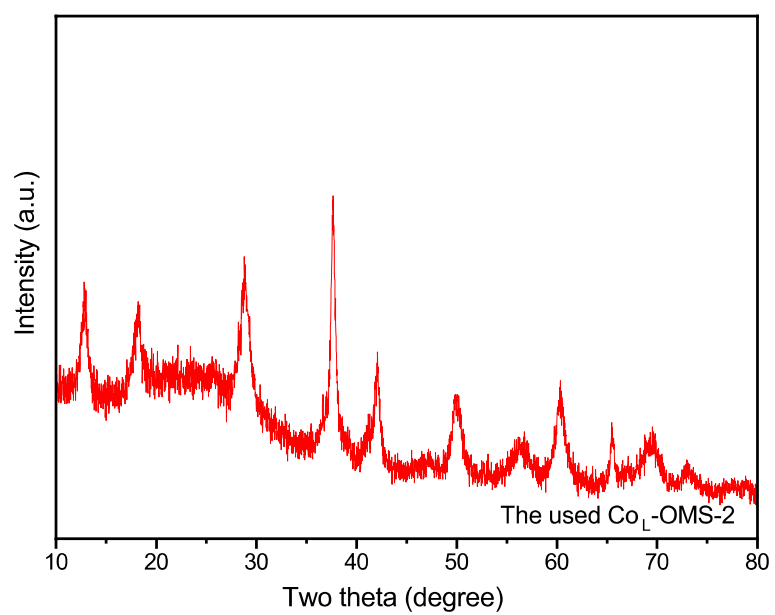


Figure S6 The XRD patterns of the used CoL-OMS-2 sample after successive reaction of 12 h at 260 °C for benzene oxidation under the condition of benzene concentration = 2000 mg m⁻³ and SV = 48000 mL g_{catal}⁻¹ h⁻¹.